Supplementary Information

Reconfigurable Microfluidics: Real-time Shaping of Virtual Channels through Hydrodynamic Forces

*David P. Taylor, Govind V. Kaigala**

Analytical modelling and reproduction of flow patterns

Analytical description of 2D flow patterns: At Reynolds numbers on the order of $5 \cdot 10^{-2}$, flow inside the flow cell is purely laminar and a streamline pattern formed on e.g. the middle plane between the bottom and the top confining surface is also formed on any other xy-plane. It is therefore enough to consider the 2D case of any xy-plane via complex potential flow theory.[36,37] The position of the m^{th} source on a corresponding complex plane is therefore given by a complex number $c_m = x_m + i \cdot y_m$. The complex potential Ω_m created by this source at any position $c = x + i \cdot y$ is

$$\Omega_m(c) = \phi + i\psi = \frac{Q_m}{2\pi} \cdot ln(c - c_m)$$

The real part of the complex potential is the velocity potential ϕ, whereas the complex part is the stream function ψ. The complex potential is created by a set of n sources and can be directly written as linear superposition of the single contributions $\Omega = \Omega_1 + ... + \Omega_n$. The complex flow velocity vector $\vec{v}(c)$ at a given position c can be conveniently derived from the complex potential $\Omega(c)$ by differentiation:

$$\vec{v}(c) = u(c) + i \cdot w(c) = \frac{d\Omega(c)}{dc^*} = \frac{d}{dc^*} \sum_{m=1}^{n} \frac{Q_m}{2\pi} \cdot ln(c - c_m)$$

Here, * denotes the complex conjugate and u and w are the velocity components along the real and the imaginary axes, respectively.

We assume all lateral walls are far enough away from virtual channels, so that we can ignore friction at these boundaries. We implement a no-flow, slip boundary condition at the walls and a zero-potential boundary condition at the opening of the flow cell by the summation of mirrored, virtual counterparts of the sources present in the system on the opposite sides of these boundaries. This is convenient as it only adds additional source terms to be considered and does otherwise not complicate the analysis.

Reproduction of user designed flow patterns: To determine the parameters required to adapt a virtual channel to a spline defined by a user, this spline is discretized at l points in the complex plane. At the k^{th} discretization point, the corresponding complex tangent vector $\vec{t}(c_k) = g_k + i \cdot h_k$ to the spline is determined, with g_k and h_k being the vector components along the real and the imaginary axes, respectively. A symbolic expression for the flow velocity vector at each discretization point can be obtained, as discussed above. The complex cross product between the tangent vector and the velocity vector returns an imaginary number, which is a measure for the area spanned by the two. In case the flow pattern generated collectively by all sources in the flow cell perfectly matches the user defined pattern,

the tangent vector and the velocity vector at all discretization points are collinear and the complex cross product is identical zero:

$$\vec{t}(c_k) \times \vec{v}(c_k) = \frac{\vec{t}^{\,*}(c_k) \cdot \vec{v}(c_k) - \vec{t}(c_k) \cdot \vec{v}^{\,*}(c_k)}{2} = 0$$

When inserting the expression for the velocity vector $\vec{v}(c)$ given above, one obtains a sum with n summands in which the m^{th} summand contains the source strength of the m^{th} source and a pre-factor a_m. Analog sum terms can be written for each discretization point and all terms can be conveniently written in matrix from by grouping the pre-factors in a coefficient matrix:

$$\begin{pmatrix} a_{11} & \cdots & a_{1n} \\ \vdots & \ddots & \vdots \\ a_{l1} & \cdots & a_{ln} \end{pmatrix} \cdot \begin{pmatrix} Q_1 \\ \vdots \\ Q_n \end{pmatrix} = \begin{pmatrix} 0 \\ \vdots \\ 0 \end{pmatrix}$$

To define a stagnation-point at a position c_k, an additional equation can be added to the above system, which simply writes as

$$\vec{v}(c_k) = \frac{d}{dc^*} \sum_{m=1}^{n} \frac{Q_m}{2\pi} \cdot ln(c_k - c_m) = 0$$

With sufficiently fine discretization the number of discretization points is much larger than the number of sources, i.e. $l \gg n$, and above system is overdetermined. We solve for the individual source strengths $Q_1 \cdots Q_n$ by a performing a conventional least-squares fit. To provide a fix reference, we choose a convenient injection flow rate for the injection from the main aperture and set this flow rate as the strength Q_1 of the first source. As the system is linear and the physical main injection flow rate is used as the reference source strength Q_1, the determined source strengths for the sources in the array can directly be set as flow rates at the corresponding apertures. The described method of matching a user defined pattern using a single least-squares fit was our method of choice, as it is straightforward to implement and provides satisfying performance in matching basic patterns, such as single lines with multiple inflection points. To match more complicated configurations such as virtual channels or multiple virtual channels, genetic algorithm might be better suited to determine the required flow rate at each source.

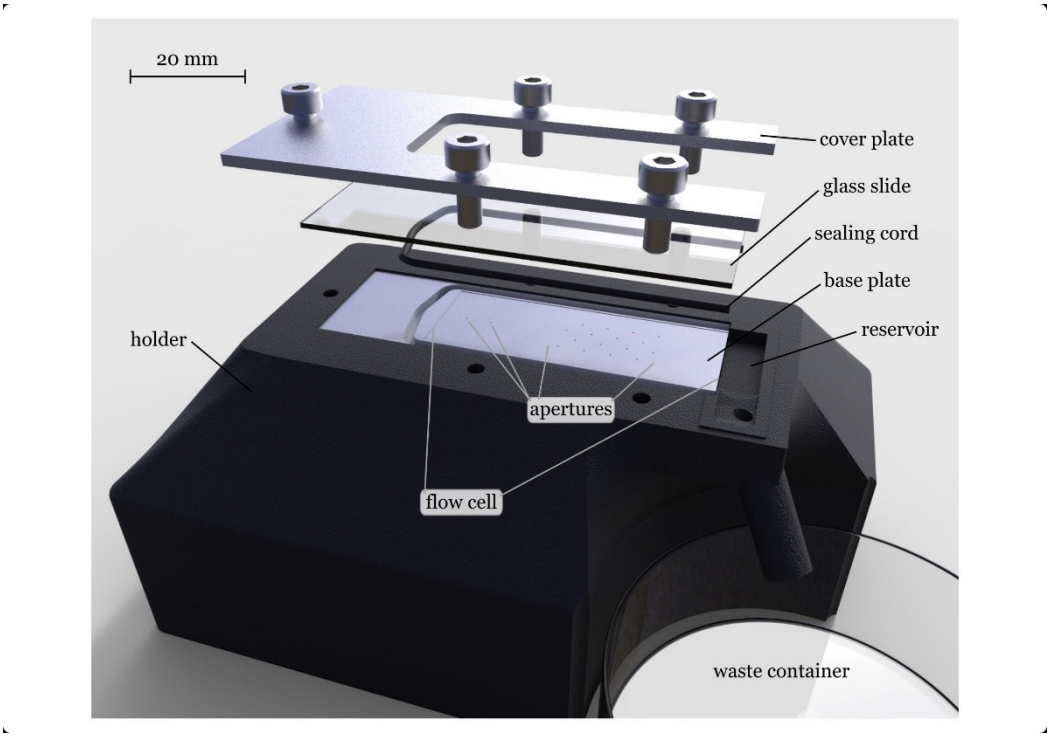

Figure S1 Flow cell assembly for generation of reconfigurable flow patterns. The aluminum base plate featuring the recess (which forms the lower part of the flow cell) and the apertures is mounted into a 3D printed holder. The holder has threads to allow the fixation of the top cover plate and fixates the capillaries which are connected to the rear side of the base plate. Further, a small reservoir at the open end of the flow cell ensures a homogeneous open boundary condition by ensuring the open boundary of the flow cell remains submersed. A glass slide is clamped on top of the base plate to close the flow cell by screwing a cover plate to the 3D printed holder. A sealing cord avoids leakage of liquid in between the base plate and the glass slide.

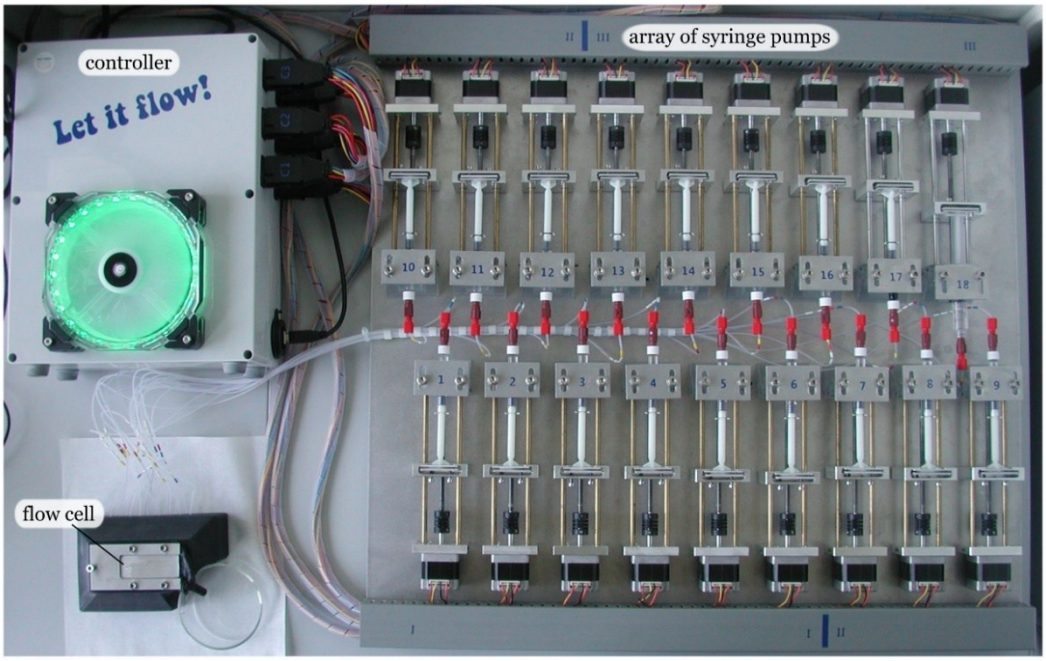

Figure S2 Array of syringe pumps for actuation of flow. In the described case, flow was actuated by an array of 18 syringe pumps, which were directly interfaced with the user interface for definition of flow patterns. Instructions to build such systems are available in literature.[38,39] We adapted a design provided by Dr. Bill Connelly (University of Tasmania) due to its simplicity: http://www.billconnelly.net/?p=176 (last accessed: Feb. 24, 2020). We used three Arduino Uno microcontroller prototyping boards, each equipped with three commercially available motor-control shields, to control the 18 bipolar stepper motors. A standard PC power supply was used to power all components.

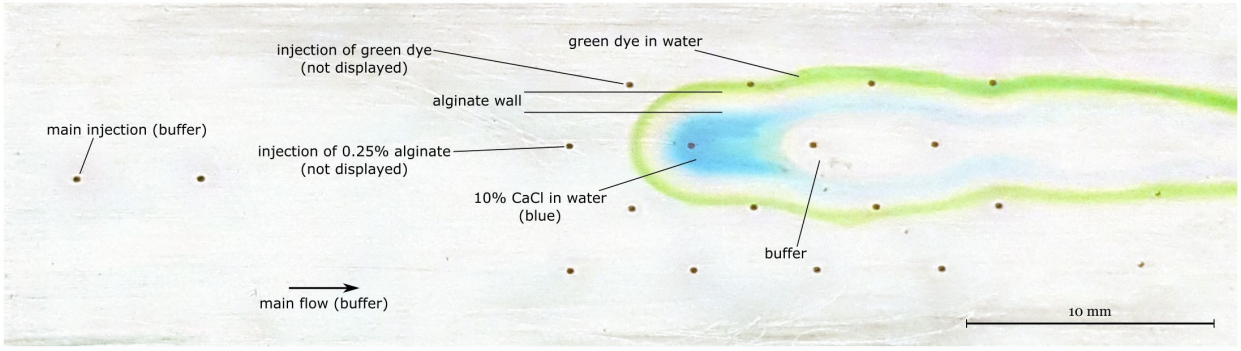

Figure S3 In-situ formation of alginate walls. After polymerization of an alginate wall at the interface between two adjacent virtual channels (the inner one containing 10% CaCl2, the outer one 0.25% sodium alginate) for 10 s, the flow cell was washed out with water. We then filled the flow cell with green food, which was subsequently flushed out with clear water again. The food dye partially diffused into the polymerized alginate wall and made it visible. This or a similar approach could be used to form in-situ semi-permeable walls in 2D flow cells for e.g. long-term cell studies. We think that it would also be interesting to flow photo-polymerizable materials in or around virtual channels, to stop all flow to suppress advection, and to then illuminate the entire flow cell to create specific microfluidic structure in analogy to established 3D printing approaches.

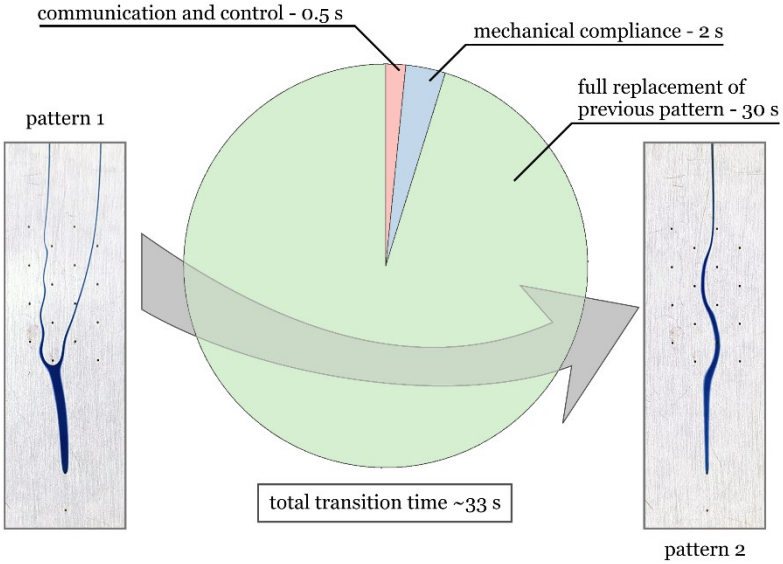

Figure S4 The transition time between two flow patterns is composed of the time required for commination between the software interface and the flow control setup (red), the time required for the flow rates to stabilize (blue) (compliance and reverse play of custom made syringe pumps), and the time required to flush the flow cell (green) to make sure the reagent is only contained in the newly formed virtual channel.

Video S1

This video illustrates a workflow to establish virtual channels implemented in the custom software interface, which we used to control our array of syringe pumps. The real-time footage of the formation of a virtual channel at the end of the video illustrates critical time constants in the demonstrated system.

Video S2

Illustration of the transitions time between different configurations of virtual channels, as well as of the splitting of virtual channels at stagnations points.

Video S3

This video demonstrates the implementation of programmed sequences of different configurations of a virtual channel, which is in this case used to move a virtual channel back and forth in a sweeping manner. By programming different speeds for different episodes of cyclic motion patterns, the incubation time of the top surface of the flow cell with a reagent contained in the virtual channel could be tuned locally.

Video S4

This video further illustrates how the presented platform could be used to e.g. perform precisely timed interactions with surface of interest by flowing “bursts” of reagents through the flow cell. Bursts of colored liquid are also useful to visualize the entirety of a flow pattern, which usually cannot be visually captured.